Geochemistry of late Quaternary tephra-sediment sequence from north-eastern Basin of Mexico (Mexico): implications to tephrochronology, chemical weathering and provenance

Priyadarsi D. Roy[1,*], José Luis Arce[1], Rufino Lozano[1], M.P. Jonathan[2], Elena Centeno[1], and Socorro Lozano[1]

[1] Instituto de Geología, Universidad Nacional Autónoma de México, Ciudad Universitaria, Del. Coyoacán, C.P. 04510, México D.F., Mexico.
[2] Centro Interdisciplinario de Investigaciones y estudios sobre Medio Ambiente y Desarrollo, Instituto Politécnico Nacional, Del. Gustavo A. Madero, C.P. 07340, México D.F., Mexico.
** roy@geologia.unam.mx*

ABSTRACT

A ca.30 m thick tephra-sediment sequence from the north-eastern Basin of Mexico (Pachuca sub-basin, central Mexico) is investigated for stratigraphy and multi-element geochemistry to understand the tephrochronology, provenance and conditions of chemical weathering during Late Quaternary. Chemical compositions of tephra layers are compared with products from surrounding volcanic structures (Apan-Tezontepece, Acoculco, Huichapan, Sierra de las Cruces and Tláloc) in order to identify their sources. Basalt to basaltic-andesite tephra layers (Tr 1, Tr 6 and Tr 7) show similar composition with rocks from Apan-Tezontepec monogenetic volcanic field aged between 1.50 and 0.47 Ma. Felsic tephra layers have composition comparable to Acoculco volcanic sequence. The dacitic ash (Tr 2) and rhyolitic ash and pumice fall deposits (Tr 3, Tr 4, Tr 5 and Tr 8) might be representatives of different Plinian eruptive events at Acoculco caldera and possibly occurred during <1.50 Ma and >0.24 Ma. Ternary diagrams (A-CN-K, A-C-N and A-CNK-FM) and trace element concentrations suggest that some of the sediment layers are formed from the chemical weathering of the underlying tephra and the rest of the inter-bedded sediments are derived from the erosion of rocks exposed at the Pachuca volcanic range. Indices of chemical weathering such as CIA and PIA indicate varying degrees of chemical alteration for these sediments possibly related to fluctuating humidity and duration of exposure to different weathering agents during their transportation from the hinterland to the sub-basin.

Key words: geochemistry, tephrochronology, provenance, chemical weathering, Quaternary, Basin of Mexico.

RESUMEN

En el presente trabajo se estudia la estratigrafía y geoquímica de multielementos de una secuencia tefro-sedimentaria localizada al noreste de la Cuenca de México (subcuenca de Pachuca, centro de México), con el fin de entender la tefrocronología, proveniencia y condiciones de intemperismo químico durante el Cuaternario Tardío. Se compara la composición química de las tefras con productos de

Roy, P.D., Arce, J.L., Lozano, R., Jonathan, M.P., Centeno, E., Lozano, S., 2012, Geochemistry of late Quaternary tephra-sediment sequence from north-eastern basin of Mexico (Mexico): implications to tephrochronology, chemical weathering and provenance: Revista Mexicana de Ciencias Geológicas, v. 29, núm. 1, p. 24-38.

estructuras volcánicas de los alrededores del área de estudio (Apan-Tezontepec, Acoculco, Huichapan, Sierra de las Cruces y Tláloc) con el fin de identificar su posible fuente. Las tefras de composición basáltica a andesita-basáltica (Tr 1, Tr 6 y Tr 7) muestran composiciones similares a las rocas del campo monogenético Apan-Tezontepec, con edades entre 1.50 y 0.47 Ma. Las tefras félsicas muestran composiciones químicas similares a las secuencias volcánicas de Acoculco. En particular, la ceniza dacítica (Tr 2), así como los depósitos de caída de pómez riolítica (Tr 3, Tr 4, Tr 5 y Tr 8) podrían representar diferentes erupciones de tipo pliniano de la caldera Acoculco, ocurridas entre <1.50 Ma y >0.24 Ma. Diagramas ternarios (A-CN-K, A-C-N y A-CNK-FM) y la concentración de elementos traza sugieren que algunos de los sedimentos intercalados son productos de alteración de las tefras y los restos de sedimentos en la secuencia provienen de la erosión de rocas que afloran en la sierra volcánica de Pachuca. Los índices de intemperismo químico como CIA y PIA indican variaciones en el grado de alteración química para estos sedimentos, posiblemente relacionado a fluctuaciones de la humedad y tiempo de su transporte desde el interior a la subcuenca.

Palabras clave: geoquímica, tefrocronología, proveniencia, intemperismo químico, Cuaternario, cuenca de México.

INTRODUCTION

Geochronological information of the Late Quaternary paleo-environmental research is mainly based on radiocarbon dating of organic matter and luminescence dating (OSL and TL) of quartz grains. However, tephrochronology or tephrostratigraphy provides an alternate method to achieve reliable chronological information for both archeological and paleo-environmental research in arid to semi-arid regions with abundant volcanic activity (Giaccio *et al.*, 2008) and correlation of different sites within the same basin. This is because of some uncertainty and complexity involved with both radiocarbon and luminescence dating methods. Radiocarbon method is unable to constrain the paleo-environmental information prior to 50 ka and most importantly, it fails in dating sediments from arid and semi-arid regions that lack organic matter. In the absence of organic matter, luminescence dating (OSL and TL) is a useful method for Quaternary geochronology (Aitken, 1985). However, this methodology needs special sampling, preparation and measurement procedures. In a recent study, González *et al.* (2006) reported the difficulties in dating volcanic material as it suffered from significant fading and caused severe age underestimates (Bonde *et al.*, 2001).

The Basin of Mexico is a topographically closed and high altitude sedimentary basin located in the central-eastern part of the Trans-Mexican Volcanic Belt (TMVB) in central Mexico (Figure 1a). Based on radiocarbon dates, the lacustrine sediments of the southern and central part of the basin (Figure 1b) were studied extensively for pollen, diatoms, mineral magnetism and sediment geochemistry to decipher the Pleistocene-Holocene paleo-environmental information (Lozano–García *et al.*, 1993; Caballero, 1997; Caballero and Ortega-Guerrero, 1998; Lozano-García and Ortega-Guerrero, 1998; Caballero *et al.*, 1999; Metcalfe *et al.*, 2000). Similarly, González *et al.* (2006) and Lamb *et al.* (2009) studied the evidence of human impact on environmental conditions in the basin. However, relatively less is known from the northern part of the basin (Roy *et al.*, 2008, 2009, 2010). Sedimentary records from different parts of the basin show the presence of Late Quaternary tephra layers. These tephra layers are products of volcanic activity from the surrounding monogenetic volcanoes and stratovolcanoes, and have potential to be used as time markers for the intra-basin paleo-environmental research, especially for correlating the arid northern part of the basin that lacks organic matter with the relatively humid south-central part. Ortega-Guerrero and Newton (1998) and Newton and Metcalfe (1999) attempted to establish tephrochronology as the basis of a geochronological framework for paleo-environmental research in central Mexico, but no substantial work has been done afterwards.

In this paper, we present geochemical data of a Late Quaternary tephra-sediment sequence from the Pachuca sub-basin to understand the past volcanic activity and strengthen the tephrochronological information from the north-eastern part of the basin. Additionally, we focus on the geochemical characterization of the sediments to understand their provenance and possible environmental conditions during their deposition using A-CN-K, (A-K)-C-N and A-CNK-FM ternary diagrams and different indices of chemical weathering.

REGIONAL SETTING

The Basin of Mexico is a high altitude (*ca.* 2240 m asl) sedimentary basin (Figure 1a) and receives varying average annual precipitation (600-700 mm/yr at north-east and 700-1000 mm/yr at south-west). The basin is limited to the north by the Pachuca volcanic range, to the southeast by the Sierra Nevada (Popocatépetl, Iztaccíhuatl, Telapón, and Tláloc volcanoes), to the south by Chichinautzin monogenetic volcanic field and to the west by Sierra de las Cruces volcanic range (Figure 1b). Though intense volcanic activity has occurred in the TMVB since the Oligocene epoch

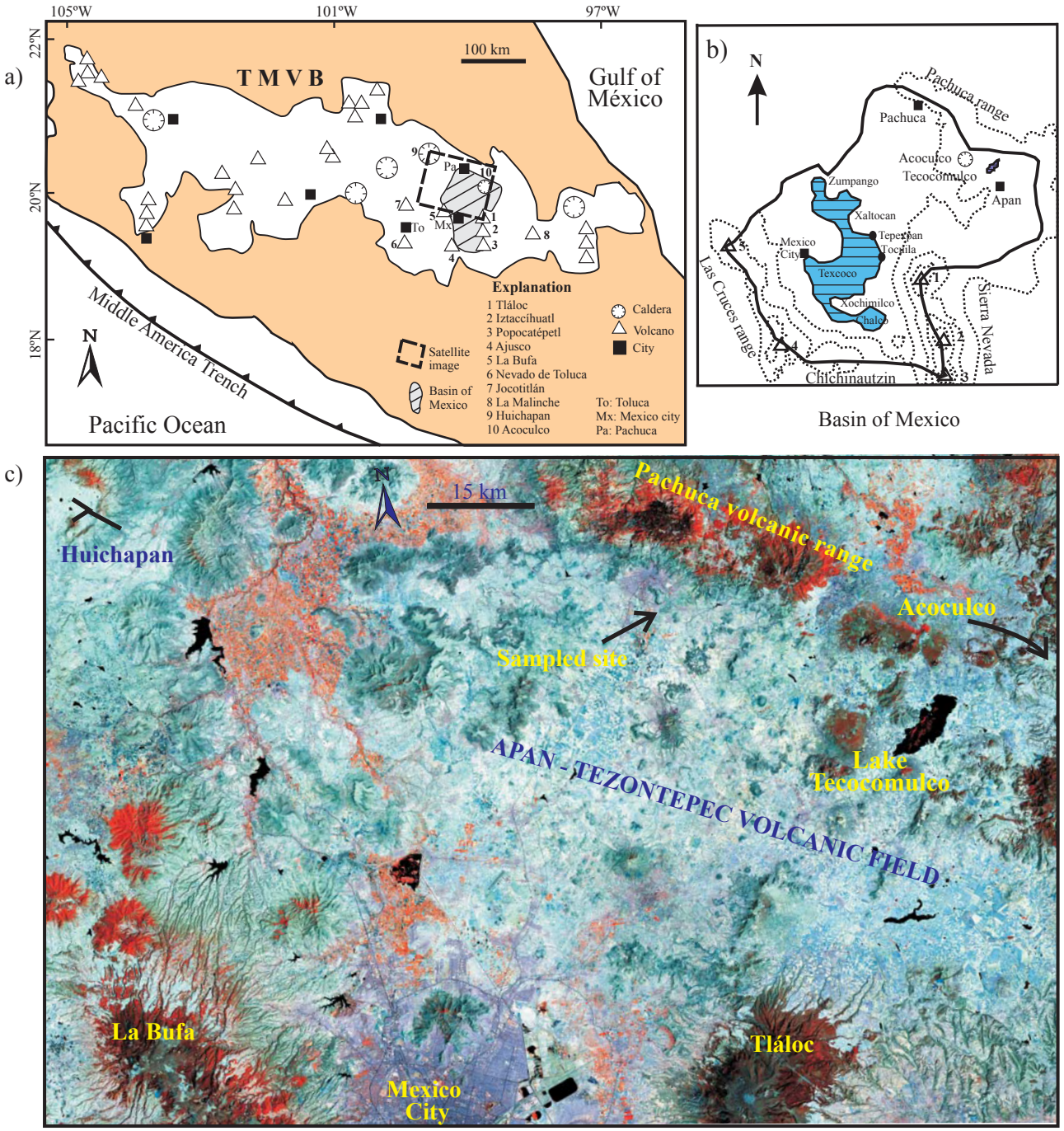

Figure 1. (a) Map showing the Trans-Mexican Volcanic Belt (TMVB) province, (b) extension of Basin of Mexico and (c) satellite image showing the location of the studied profile in the Pachuca sub-basin, as well as the some volcanic structures mentioned in the text.

(Ortega-Guerrero and Newton, 1998), the topographically closed nature of the Basin of Mexico is associated with the formation of the Chichinautzin volcanic field in the Late Quaternary (0.78 Ma) (Mooser *et al.*, 1974; Urrutia and Martín del Pozzo, 1993). Presently, the basin hosts a number of relict sedimentary sub-basins: Xochimilco and Chalco in the south, Texcoco in the centre, Zumpango and Xaltocan in the north, and Tecocomulco and Pachuca in the north-east (Figure 1b).

The sub-basin of Pachuca is located in the central-eastern sector of the TMVB where volcanism started during 30-20 Ma (Mooser *et al.*, 1974; Cantagrel and Robin, 1979) and is surrounded by a number of monogenetic and polygenetic volcanoes (Figure 1c). The Apan-Tezontepec monogenetic volcanic field (ATVF) is represented by at least 295 volcanic structures (scoria cones, shield volcanoes and domes) with basalt to basaltic-andesite lava flow, ash and scoria fallouts (García-Palomo *et al.*, 2002) constrained

between 1.50 and 0.47 Ma (Cantagrel and Robin, 1979; López-Hernández and Castillo-Hernández, 1997; García-Palomo *et al.*, 2002). These mafic eruptions might have obstructed the existing drainage and formed the endorreic Pachuca sub-basin.

The semi-rectangular caldera of Huichapan with a *ca.* 10 km wide depression is located at a distance of 87 km to the west of Pachuca. Two important caldera related eruptions of andesitic to trachydacitic pyroclastic flows and rhyolitic tuffs are dated to 5.0 and 4.2 Ma, respectively (Aguirre-Díaz and López-Martínez, 2009). The semi-circular Acoculco caldera is located at a distance of 33 km to the south-east (López-Hernández *et al.*, 2009) and has an intense eruptive history ranging in composition between basaltic-andesite and rhyolite during 3.0-0.24 Ma (López-Hernández and Castillo-Hernández, 1997). One of the biggest eruptions responsible for the collapse of the structure took place at *ca.* 1.4 Ma and deposited a rhyolitic tuff (López-Hernández, 2009). Tláloc is a stratovolcano and forms the northernmost part of the Sierra Nevada volcanic chain. It is present at a distance of 74 km towards south of the study area. The main structure of the volcano is of Pliocene in age (García-Palomo *et al.*, 2002) with pumice flows and fallout deposits continuing during Pleistocene, with the recent eruptions at *ca.* 44 and *ca.* 31 ka ^{14}C BP, respectively (Rueda *et al.*, 2006, 2007). Chemical compositions of Tláloc products display a continuous range of silica contents, *i.e.* andesite, dacite and rhyolite.

The northern end of Sierra de las Cruces volcanic range is represented by the La Bufa volcano (García-Palomo *et al.*, 2008), located at a distance of 100 km to the south-west. This is a complex structure dated at 3.7 Ma (Osete *et al.*, 2000). Available geochemical analyses from La Bufa and the northern sector of Sierra de las Cruces show compositions ranging between andesite and dacite (Rodríguez-Saavedra, 2007). Apart from the Quaternary volcanoes and their products, Tertiary extrusive igneous rocks are exposed in different formations in the Pachuca volcanic range (Geyne *et al.*, 1963). The rocks of San Cristóbal Fm. comprise basaltic-andesite, whereas the rocks from Corteza, Pachuca, Real del Monte, Santa Gertrudis, Vizcaína and Zumate Fms. consist of andesites. The volcanic deposits of Santiago and Tezuantle Fm. contain rhyolites and deposits of Cerezo Fm. are dacitic in nature.

Tephrochronological information of the basin

Tephra layers were studied in detail from the southern and central part of the TMVB and Basin of Mexico. Ortega-Guerrero and Newton (1998) reported the geochemical compositions of tephra layers ranging in age from 34 ka ^{14}C BP to 2.6 ka ^{14}C yr BP in the Chalco and Texcoco lakes. The 34 ka ^{14}C BP basaltic-andesite Tláhuac tephra, 15-14.4 ka ^{14}C BP andesite-rhyolite tephra and 14.3 ka ^{14}C BP basaltic-andesite tephra layers were sourced from Popocatéptl volcano. The 11-12 ka ^{14}C BP rhyolitic pumice from the Nevado de Toluca is also identified in the deposits of Chalco (Bloomfield *et al.*, 1977; Newton and Metcalfe, 1999). Gonzalez and Huddart (2007) and Lamb *et al.* (2009) reported the geochemistry of tephra layers from Tocuila and Tepexpan paleo-indian sites (adjacent to Texcoco lake) and suggested that most of the tephra were reworked and the *ca.* 0.5 ka ^{14}C BP basaltic-andesite and andesite tephra layer could be from one of the adjacent monogenetic cinder cones.

Information on tephrochronology from the north-eastern part is relatively scarce, except for the geochemical characterization of two distinct tephra layers present in the Tecocomulco lake (Roy *et al.*, 2008, 2009), a mafic tephra layer at Pachuca sub-basin (Roy *et al.*, 2010) and volcanic deposits of the Apan region (García-Palomo *et al.*, 2002). The *ca.* 50 ka ^{14}C BP dacite-rhyolite tephra and *ca.* 31 ka ^{14}C BP rhyolitic tephra from the lacustrine deposits of the Tecocomulco lake were sourced from the Acoculco caldera and Tláloc volcano, respectively. Additional information on tephrochronology comes from the Toluca basin, located to the south of Basin of Mexico. These tephra layers range between *ca.* 25 and 8.5 ka ^{14}C BP (Newton and Metcalfe, 1999).

MATERIAL AND METHODS

A *ca.* 30 m thick tephra-sediment sequence exposed in different parts of a mine in the Pachuca sub-basin (Figure 1c) was studied for sediment stratigraphy and multi-element geochemistry. For the geochemical analyses, 44 samples (26 samples from tephra layers and 18 samples from inter-bedded sediments) were collected and subjected to oven drying at 40°C, homogenized and grinded to 200 mesh (<0.074 mm) sizes using an agate mortar. Multi-element concentrations (major elements in weight % and trace elements in ppm) were measured in a Siemens SRS 3000 wavelength dispersive X-ray fluorescence (XRF) spectrometer after the methods of Guevara *et al.* (2005) and Lozano and Bernal (2005) at the Instituto de Geología, Universidad Nacional Autónoma de México. Major element oxides (SiO_2, Al_2O_3, TiO_2, Fe_2O_3, CaO, MgO, Na_2O, K_2O, MnO and P_2O_5) were measured in fused discs after determining the lost on ignition (LoI) by heating the sample up to 1000°C; trace elements were measured in the pressed pellets. The accuracy and precision of the analytical methods were established using international standards (QLO-1 and JA-2) and in-house reference material (BCU-3). XRF measurements have precisions up to 1.5 % for major elements and 6 % for trace elements. The accuracy for major and trace elements are 2 % and 9.5 %, respectively. Geochemical compositions of the volcanic rocks exposed in the Pachuca volcanic range are taken from Geyne *et al.* (1963). Bulk rock chemical analyses from Huichapan, Acoculco, Tláloc, Sierra de las Cruces, and ATVF are taken from several authors (García-Palomo *et al.*, 2002; Meier, 2007; Rodríguez-Saavedra,

2007; Quintanilla-Garza, 2008; Aguirre-Díaz and López-Martínez, 2009; López-Hernández, 2009; Roy *et al.*, 2009).

RESULTS

Stratigraphy

The sequence (Figure 2) consists of at least eight different tephra layers (Tr 1 to Tr 8 from bottom to top) and inter-bedded sediments (S 1 to S 6 from bottom to top). The bottommost tephra layer (Tr 1) has a thickness of 2.8 m and consists of black-brown multilayered lapilli to coarse ash scoria fallout deposits. It is characterized by granulometrically fining upward sequences. Each sequence begins with coarse grained and dark colored lapilli and terminates with coarse ash. Tr 1 has an erosive contact with the overlying sediments, *i.e.* S 1. S 1 consists of massive pale-brown sandy-silt and partly indurate fine sand. A massive beige color 3 m thick fine-medium volcanic ash deposit (Tr 2) overlies S 1 with a sharp contact. The overlying massive pale-brown sediment (S 2) has a gradual contact with Tr 2 and has a thickness of 2 m.

Tr 3 has a thickness of 0.6 m and is a white-beige color,

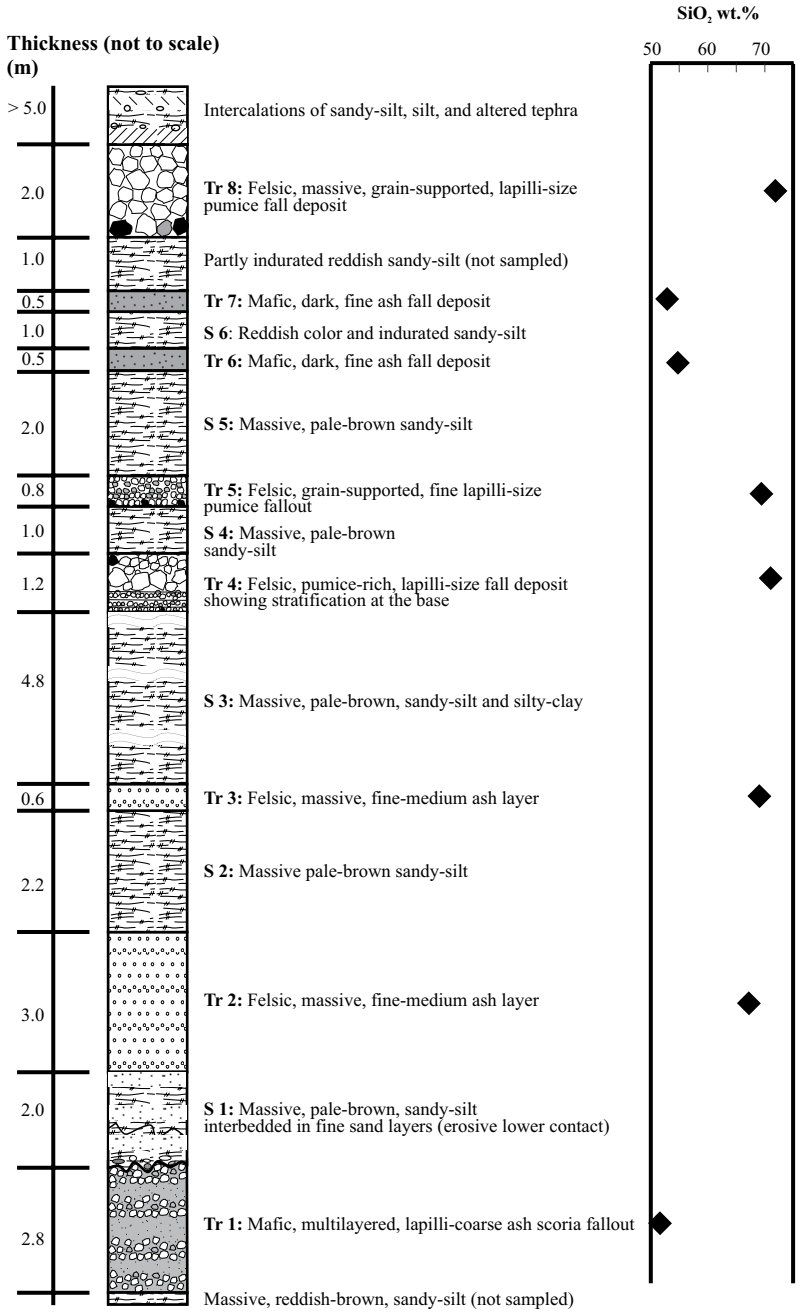

Figure 2. General stratigraphic column of the ca.30 m thick tephra-sediment sequence from the Pachuca sub-basin. T, tephra; S, sediment. Average SiO_2 content of the tephra layers are shown.

massive fine-medium ash fall deposit. This is overlain by ca. 4.8 m thick pale-brown sandy-silt and silty-clay intercalations (S 3) with an abrupt contact. Both Tr 4 (1.2 m thick) and Tr 5 (0.8 m thick) are light gray in color and consist of grain supported pumice rich, lapilli size fall deposits. They are separated by a pale brown massive silty-sand (S 4) showing an abrupt contact with Tr 4. Unlike Tr 5 which is massive, Tr 4 shows stratified base and massive top. Tr 5 is overlain by a 2 m thick massive sandy-silt (S 5). Both Tr 6 and Tr 7 have similar characteristics and comprise of dark colored coarse to fine ash fall deposits. Both are separated by a brown massive sandy-silt sediment layer (S 6) showing an abrupt contact with Tr 6. A massive 2 m thick, grain supported, lapilli sized pumice fall deposit (Tr 8) overlies *ca.* 1m thick reddish silty-sand (could not be sampled). This is capped by a >5 m thick sequence consisting of altered tephra, sandy-silt and silt intercalations.

Geochemistry

Geochemistry of tephra layers

Chemical composition. Tephra layers range in composition from basalt to rhyolite (Figure 3a) and are sub-alkaline (Figure 3b) in nature. Based on their major element compositions, tephra layers are divided into three different groups. The first group (I) consists of basalt to basaltic-andesite Tr 1, Tr 6 and Tr 7. The second group (II) has Tr 2 that ranges between andesite to rhyolite with majority of the samples falling within the dacite field. The third group (III) comprises rhyolitic Tr 3, Tr 4, Tr 5 and Tr 8.

The basalt to basaltic-andesite tephra layers have SiO_2 concentrations of 49.54-57.15 wt. % and total alkalis (Na_2O+K_2O) concentrations of 2.32-4.32 wt. %. The rhyolitic tephra layers have SiO_2 contents of 69.03-71.87 wt. % and 8.44-10.18 wt. % of total alkalis. The andesite to rhyolite tephra (Tr 2) has an intermediate chemical composition (SiO_2: 62.73-70.52 wt. % and Na_2O+K_2O: 5.01-7.73 wt. %) compared to both the above mentioned groups. Figures 3c to 3f show the bivariate plot of SiO_2 *vs*. Al_2O_3, SiO_2 *vs*. CaO, SiO_2 *vs*. MgO, and SiO_2 *vs*. TiO_2 of the tephra layers and products of the surrounding volcanoes. Basalt to basaltic-andesite tephra layers (Tr 1, Tr 6 and Tr 7) have CaO, Al_2O_3, SiO_2 and TiO_2 concentrations comparable to volcanic products from ATVF. Similarly, basaltic-andesite Tr 7 has MgO concentrations similar to rocks from Sierra de la Cruces. Both Tr 2 and Tr 3 have Al_2O_3 contents similar to Acoculco volcanic products, whereas Tr 4, Tr 5 and Tr 8 have Al_2O_3 values comparable to products from both Huichapan and Acoculco. Dacite to rhyolitic tephra layers (Tr 2, Tr 3, Tr 4 and Tr 5) have CaO and TiO_2 concentrations comparable to Tlaloc, Acoculco and Huichapan volcanic products.

Table 1 presents the average major and trace element concentrations of the tephra layers and volcanic products from ATVF, Huichapan, Acoculco, Sierra de las Cruces and Tláloc. Mafic tephra layers with composition varying between basalt and basaltic-andesite show higher concentrations of Sr, V, Cr, Co, Ni and Cu, whereas felsic tephra layers with composition varying between dacite and rhyolite have higher abundance of Rb, Y, Zr, Nb, Zn, Th and Pb.

A-CN-K diagram. The molar proportions of Al_2O_3, CaO*+Na_2O and K_2O in the tephra layers are presented in the A-CN-K triangle (Figure 4a) (Al_2O_3 plotted as top apex (A), CaO*+Na_2O at the bottom left (CN) and K_2O at the bottom right (K)) of Nesbitt and Young (1984, 1989) to understand their weathering trends and mineralogical compositions. CaO* is the concentration of CaO in silicates and corrected for apatite and carbonate contents (Fedo *et al.*, 1995). A quantitative estimation of the degree of chemical alteration of the tephra layers are obtained by calculating the Chemical Index of Alteration ($CIA = [Al_2O_3 / (Al_2O_3+CaO^*+Na_2O+K_2O)] \times 100$) as suggested by Nesbitt and Young (1982). The CIA values are indicated by the height of the sample above the baseline of the triangular diagram (Figure 4a).

CIA provides a dimensionless number that estimates the ratio of secondary aluminous minerals (clay minerals) to feldspars. Most unaltered rocks and primary minerals (feldspars and biotite) plot on or close to the feldspar join (50-50 line in the A-CN-K triangle) and have CIA values near 50. However, mafic and ultramafic rocks and minerals like amphiboles and pyroxenes have lower CIA values and plot much below the feldspar join (Young, 2001). By contrast, the secondary products have CIA values of 70-85 for smectite and illite and 100 for kaolinite group minerals and chlorite (Nesbitt and Wilson, 1992). The samples with CIA < 60 suggest lower weathering, 60-80 moderate weathering and > 80 extreme weathering (Fedo *et al.*, 1995). In the A-CN-K diagram, both parent material and their altered products fall along the same linear trend and the projection of this linear trend onto the feldspar join suggests the chemical composition and mineralogical association of the possible parental material.

The CIA values of tephra layers are presented in Table 1 and Figure 4a. Except for Tr 2, tephra layers have CIA values between 42 and 51 suggesting their unweathered nature. CIA of Tr 2 ranges between 51 and 62 and suggests lower chemical alteration. In the A-CN-K triangle, the tephra samples fall in different linear arrays sub-parallel to the A-CN join (solid line with arrow) and the projection of these linear trends onto the feldspar join suggest their feldspar assemblage. The first linear array (1) consists of basalt to basaltic-andesite Tr 1, Tr 6 and Tr 7 and its projection onto the feldspar join suggests presence of abundant plagioclase and possible absence of K-feldspar. Compared to Tr 6 and Tr 7, Tr 1 plots more towards the CaO*+Na_2O apex below the feldspar join. This could be due to higher abundance of other Ca-Na-bearing silicates, *e.g.* amphiboles and pyroxenes. The dacitic Tr 2 constitutes the second linear array (2) and consist of plagioclase>K-feldspar. The rhyolitic Tr 3, Tr 4, Tr 5 and Tr 8 have higher abundance of K-feldspar (array 3). The K-feldspar content in Tr 3 is lower compared

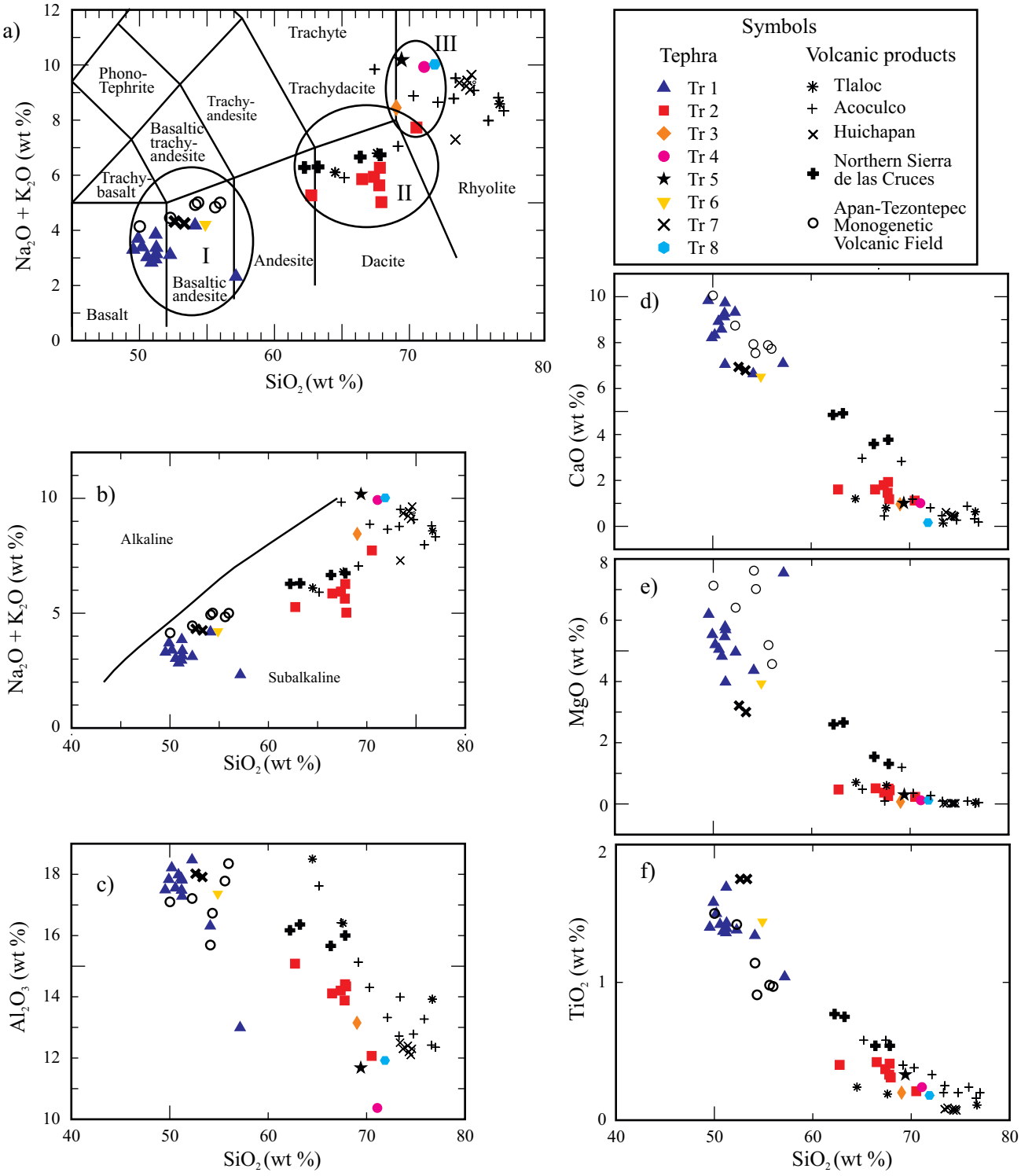

Figure 3. (a) Chemical classification diagram of total alkalis *vs.* silica (TAS) and (b to f) bivariate plots of the tephra layers present in the studied profile and volcanic rocks exposed in its surroundings. Bulk rock chemical data of the surrounding volcanic structures were taken from several authors (see Table 1).

to the rest. Compared to Tr 8, both Tr 4 and Tr 5 are plotted towards CN apex.

A-C-N diagram. Molar proportions of Al_2O_3 (minus Al associated with K), CaO* and Na_2O are plotted in the A-C-N triangle (Figure 4b) (Al_2O_3-K_2O at upper apex, CaO* at left bottom and Na_2O at right bottom) of Fedo *et al.* (1995) to understand trends of plagioclase weathering in tephra layers. Quantitative estimation of the plagioclase weathering is measured by calculating the Plagioclase Index of Alteration (PIA= [(Al_2O_3-K_2O) / (Al_2O_3+CaO*+Na_2O-K_2O)] × 100)

Table 1. Average composition (major elements in % and trace elements in ppm) and indices of chemical weathering of the tephra layers from Pachuca sub basin and volcanic products from surrounding volcanoes.

	Tr 1	**Tr 2**	**Tr 3**	**Tr 4**	**Tr 5**	**Tr 6**	**Tr 7**	**Tr 8**	**Huichapan[1]**	**Sierra de las Cruces[2,6]**	**Acoculco[3]**	**Tláloc[4]**	**ATVF[5]**
	n=12	n=7	n=1	n=1	n=1	n=1	n=2	n=1	N=7	N=4	n=11	N=3	N=6
SiO_2	51.63	67.23	69.03	71.09	69.41	54.88	52.97	71.87	74.21	64.91	72.28	77.12	53.72
TiO_2	1.41	0.35	0.20	0.24	0.33	1.44	1.75	0.18	0.08	0.65	0.32	0.10	1.15
Al_2O_3	17.27	14.00	13.15	10.37	11.68	17.36	18.02	11.92	12.30	16.05	14.03	13.74	17.14
Fe_2O_3	8.30	4.24	3.18	2.55	2.07	8.70	9.21	2.19	1.22	4.18	1.33	0.84	7.64
MnO	0.12	0.07	0.07	0.12	0.08	0.12	0.13	0.12	0.02	0.07	0.05	0.06	0.11
MgO	5.38	0.38	0.07	0.12	0.30	3.93	3.10	0.12	0.02	2.03	0.24	0.09	6.32
CaO	8.51	1.51	0.96	1.01	1.01	6.51	6.87	0.16	0.44	4.28	0.95	0.57	8.31
Na_2O	2.65	2.54	3.22	2.81	2.66	3.00	3.27	3.10	2.34	4.42	4.13	3.15	3.58
K_2O	0.61	3.40	5.23	7.12	7.52	1.21	1.01	6.92	6.72	2.08	4.31	5.25	1.15
P_2O_5	0.23	0.03	0.01	0.02	0.02	0.20	0.32	0.01	0.01	0.19	0.03	0.01	0.28
LoI	3.89	6.76	5.36	4.91	4.53	2.56	3.27	3.30	-	-	-	3.14	-
Rb	17	95	127	228	172	39	25	330	-	39	-	166	18
Sr	630	208	76	18	32	564	648	14	-	454	-	44	556
Ba	308	843	1009	5	170	383	412	59	-	379	-	321	336
Y	23	54	57	109	117	28	26	66	-	15	-	21	19
Zr	162	479	480	1035	720	213	225	764	-	137	-	56	-
Nb	13	34	43	10	67	17	15	115	-	9	-	11	-
V	199	22	bdl	6	4	115	138	2	-	75	-	61	159
Cr	138	7	bdl	bdl	bdl	29	26	bdl	-	165	-	6	169
Co	40	12	4	12	34	38	31	bdl	-	15	-	-	53
Ni	35	12	10	6	11	31	22	3	-	50	-	2	102
Cu	17	3	bdl	bdl	7	20	11	bdl	-	20	-	0	20
Zn	78	152	181	241	173	98	110	165	-	85	-	30	70
Th	3	11	15	22	14	bdl	bdl	47	-	3	-	-	3
Pb	4	18	21	26	18	bdl	8	40	-	9	-	49	5
CIA	44-51	51-62	51	42	45	50	49-50	48	49-58	48-50	50-56	54-65	42-47
PIA	43-51	51-66	52	29	36	50	49-50	45	49-67	48-50	50-57	58-70	41-46

[1]Aguirre-Diáz and López-Martínez, 2009; [2]Rodríguez-Saavedra, 2007; [3]López-Hernández, 2009; [4] Meier, 2007; [4]Roy *et al.*, 2009; [5]García-Palomo et al, 2002; [6]Quintanilla-Garza, 2008. bdl: below detection limit.

of Fedo *et al.* (1995) and presented in Table 1.

Both the PIA and CIA values are comparable. Basalt to basaltic-andesite tephra layers (Tr 1, Tr 6 and Tr 7) show PIA values between 43 and 51, whereas dacitic tephra layers (Tr 2) have PIA values of 51-66. Rhyolitic tephra layers (Tr 3, Tr 4, Tr 5 and Tr 8) have lower PIA values (29-52) compared to the rest. The plagioclase weathering trends suggest enrichment of anorthite in the mafic tephra layers and albite in the felsic tephra layers (Figure 4b). With increasing PIA, mafic tephra layers are depleted in CaO* and felsic tephra layers in Na_2O. This suggests that with gradual increase in chemical weathering, the tephra layers are depleted in both anorthite and albite and enriched in secondary aluminous clay minerals. The relatively higher CaO* in Tr 1 compared to both Tr 6 and Tr 7 suggest that the amphiboles and pyroxenes in Tr 1 are Ca-bearing. Similarly, the higher Na_2O in Tr 4 (PIA=29) and Tr 5 (PIA=36) suggest presence of some other Na-bearing constituent, *e.g.* glass fragments.

A-CNK-FM diagram. Figure 4c shows the molar proportions of Al_2O_3 (A), CaO*+Na_2O+K_2O (CNK) and Fe_2O_3+MgO (FM) in the ternary diagram of Nesbitt and Wilson (1992). Except for Tr 2, all the tephra layers fall long the linear array joining Feldspars (Fs) with FM apex. However, the mafic tephra layers (Tr 1, Tr 6 and Tr 7) plot away from the feldspars suggesting higher abundance of mafic minerals, *e.g.* olivine, pyroxene and amphibole. Rhyolitic tephra layers (Tr 4 and Tr 5) plot towards the CNK apex and suggest higher abundance of CaO*, Na_2O and K_2O. The relatively weathered dacitic tephra (Tr 2) plots within the feldspars (Fs), kaolinite (Ka) and smectite (Sm) compositional triangle. Except for few samples, they lie much closer to feldspars along the Fs-Sm join. This suggests that feldspars and smectite are more abundant than kaolinite. Few samples of Tr 2 plot above the Fs-Sm line and suggest presence of kaolinite (< 20 %).

Geochemistry of sediments

Chemical composition. Based on their major and trace element compositions, the sediments are divided into three different groups. The first group consists of S 2 and S 5 with

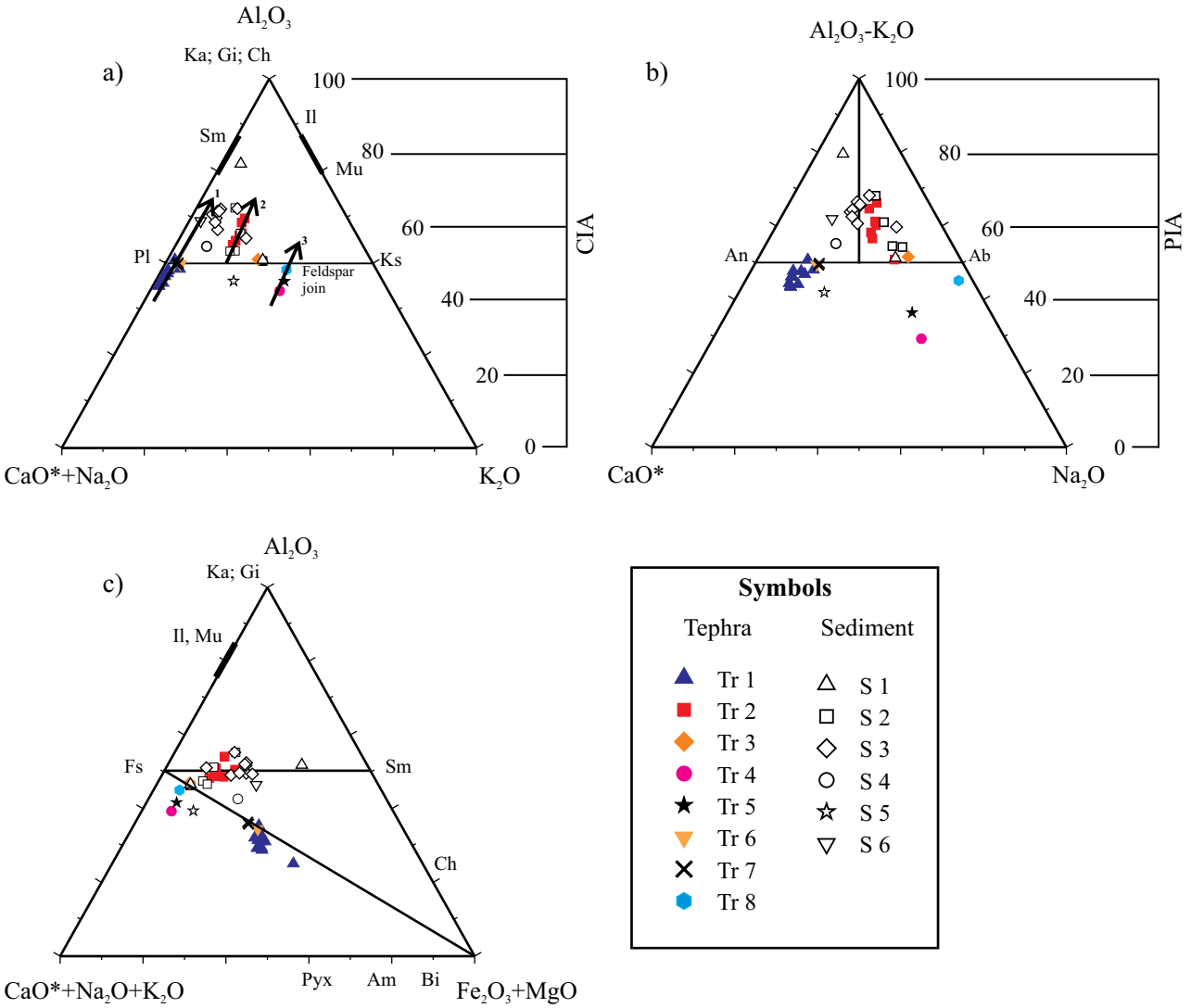

Figure 4. (a) Major element compositions of the tephra and sediments plotted as molar proportions on an Al_2O_3-(CaO^*+Na_2O)-K_2O (A-CN-K) diagram. Arrows indicate weathering trend of the tephra samples. The scale showing the chemical index of alteration (CIA) is shown at the right side. (b) Ternary diagram (A-C-N) showing molar proportions of Al_2O_3 (substracting the Al associated with K), CaO^* and Na_2O in the tephra and sediment samples. The scale showing the plagioclase index of alteration (PIA) is shown at the right side. (c) Ternary diagram (A-CNK-FM) showing the molar proportions of Al_2O_3, $CaO^*+Na_2O+K_2O$ and Fe_2O_3+MgO in the tephra and sediments. The diagram represents the fields of idealised minerals: Pl, plagioclases; Ks, K-feldspars; Il, illite; Mu, muscovite; Sm, smectite; Ka, kaolinite; Gi, gibbsite; Ch, chlorite; An, anorthite; Ab, albite; Fs, feldspars; Pyx, pyroxene; Am, amphibole; Bi, biotite.

higher concentrations of SiO_2, K_2O, Rb, Y, Zr, Zn, Th and Pb. Second group comprises S 4 and S 6 and show higher abundance of Al_2O_3, TiO_2, Fe_2O_3, MgO, CaO, P_2O_5, Sr, Cu, Cr and Ni. Except for few samples of S 2, both the groups have comparable MnO and Na_2O concentrations. Ba does not show any significant pattern. The third group consists of S 1 and S 3 and show large variation in the concentrations of both major and trace elements. The concentration range covers the concentrations of both the above mentioned groups. Table 2 presents the average composition of the sediments and the rocks exposed in the Pachuca volcanic range.

A-CN-K diagram. The CIA values of sediments are presented in Table 2. Except for S 5, CIA of sediments vary between 53 and 77 suggesting low to intermediate chemical alteration of the parent material. The CIA value of S 5 (CIA=45) suggests absence of chemical alteration. In the A-CN-K ternary space (Figure 4a), the sediments fall along different linear arrays. S 5 plots below the feldspar join towards the CaO*+Na2O apex suggesting its higher abundance of amphiboles and pyroxenes. S 4, S 6 and some samples of S 1 and S 3 show higher abundance of plagioclase, whereas S 2 and some samples from S 1 and S 3 are characterized by presence of both K-feldspar and plagioclase.

It is interesting to note that most of the sediments do not fall along the linear trend that contains their underlying tephra layer, except for S 6 (linear trends 1 in Figure 4a). These sediments and their underlying tephra layer fall in

Table 2. Average composition (major elements in % and trace elements in ppm) and indices of chemical weathering of the sediments from Pachuca sub basin and rocks exposed in the sierra de Pachuca (Geyne *et al.*, 1963).

	sediments						basaltic-andesite	andesite						dacite	rhyolite	
	S1 n=2	S2 n=4	S3 n=9	S4 n=1	S5 n=1	S6 n=1	San Cristóbal	Corteza	Pachuca	Real de Monte	Santa Gertrudis	Vizcaína	Zumate	Cerezo	Santiago	Tezuantle
SiO_2	62.46	66.46	62.74	61.89	64.41	53.13	52.90	59.20	60.80	60.25	60.10	60.80	60.40	69.80	72.13	75.20
TiO_2	0.56	0.35	0.80	1.03	0.39	1.82	1.86	1.20	0.84	0.84	0.73	0.89	0.88	0.52	0.41	0.19
Al_2O_3	15.53	14.75	16.48	15.89	12.74	19.84	18.20	16.20	15.80	16.40	15.40	16.10	15.60	13.45	12.90	11.90
Fe_2O_3	4.97	4.23	5.31	6.23	3.09	10.20	9.10	6.00	4.90	4.90	4.80	4.80	4.90	3.30	3.42	2.70
MnO	0.04	0.08	0.10	0.08	0.10	0.13	0.14	0.10	0.08	0.09	0.06	0.07	0.07	0.03	0.06	0.01
MgO	1.47	0.38	0.94	1.64	0.84	1.51	4.60	3.40	3.50	2.85	3.00	2.70	2.80	0.90	0.23	0.40
CaO	1.40	1.35	2.20	3.84	3.63	4.40	7.60	5.40	5.70	5.15	4.90	6.30	5.10	2.60	0.56	0.40
Na_2O	1.81	3.19	2.54	2.57	2.24	2.39	3.80	2.80	3.30	3.45	3.90	3.10	3.90	3.40	2.87	2.20
K_2O	3.20	3.13	1.85	2.06	4.95	0.82	1.00	2.60	2.20	1.70	1.00	1.40	1.90	2.50	5.80	4.30
P_2O_5	0.03	0.03	0.06	0.07	0.04	0.13	0.12	0.33	0.24	0.23	0.18	0.23	0.18	0.08	0.05	0.00
LoI	8.88	6.09	7.17	4.91	6.86	4.99										
Rb	103	87	72	72	140	38	-	-	-	-	-	-	-	-	-	-
Sr	170	186	316	450	181	537	-	-	-	-	-	-	-	-	-	-
Ba	255	900	659	337	233	514	-	-	-	-	-	-	-	-	-	-
Y	43	43	35	50	68	27	-	-	-	-	-	-	-	-	-	-
Zr	264	518	396	465	838	276	-	-	-	-	-	-	-	-	-	-
Nb	27	41	26	29	67	24	-	-	-	-	-	-	-	-	-	-
V	43	17	65	65	18	168	-	-	-	-	-	-	-	-	-	-
Cr	50	9	26	38	3	43	-	-	-	-	-	-	-	-	-	-
Co	8	6	14	19	7	34	-	-	-	-	-	-	-	-	-	-
Ni	17	12	17	17	13	31	-	-	-	-	-	-	-	-	-	-
Cu	10	2	8	15	9	13	-	-	-	-	-	-	-	-	-	-
Zn	120	139	98	100	151	113	-	-	-	-	-	-	-	-	-	-
Th	8	10	8	10	15	bdl	-	-	-	-	-	-	-	-	-	-
Pb	13	20	14	7	22	6	-	-	-	-	-	-	-	-	-	-
CIA	55-77	53-65	57-65	54	45	61	47	50	47	50	49	48	47	51	52	57
PIA	51-80	54-68	60-68	55	42	62	46	50	47	50	49	48	47	51	54	63

different linear arrays. S 6 shows higher CIA compared to Tr 6 (Tables 1 and 2) and this suggests that S 6 is possibly produced by the geochemical alteration of underlying tephra layer Tr 6.

In order to understand the provenance of rest of the sediments, both sediments and rocks exposed in the Pachuca volcanic range are presented in a different A-CN-K space (Figure 5a). The linear array (i) consisting of S 4 and parts of both S 1 and S 3 projects onto the feldspar join suggesting parent material comparable to andesites from Pachuca, Real de Monte, Zumate and Vizcaína Formations. The linear trend (ii) consisting of parts of samples from S 1, S 2 and S 3 intersects the feldspar join and suggests a parent material similar to rhyolites from Santiago and Tezuantle Formations. The linear array (iii) consisting of some samples from S 2 and S 3 suggest a parent material more felsic than dacites of Cerezo Formation.

A-C-N diagram. Except for S 5, sediments have PIA values between 51 and 80. S 5 exhibits a PIA value of 42. In the A-C-N ternary space (Figure 5b), S 4 and S 6 and some samples of S 1 and S 3 show the presence of anorthite and display a linear trend with parental material comparable to andesites of Pachuca volcanic range. Although present along the same trend, S5 show higher CaO* concentration compared to the andesites possibly associated with pyroxenes and amphiboles. With gradual increase in chemical alteration, they are enriched in Al_2O_3 at the expense of CaO*. Similarly, S 2 and some samples from S 1 and S 3 have higher abundance of albite and are present along a linear trend suggesting parental material with compositions intermediate to dacite and rhylites of Pachuca volcanic range. Table 2 presents the PIA values of rocks exposed in the Pachuca volcanic range and sediments of the studied profile.

A-CNK-FM diagram. Figure 4c shows the distribution of sediments and tephra layers in the A-CNK-FM ternary diagram and Figure 5c shows the distributions of sediments with respect to the rocks exposed in the Pachuca volcanic range in a different A-CNK-FM diagram. Except for the rhyolite of Tezuantle Fm., all the rocks are present along the linear array joining feldspars with FM apex. The basaltic-andesite and andesites fall away from the feldspar apex and suggest higher abundance of mafic minerals. The dacite and rhyolite plot close to the feldspar apex and in-

dicate higher abundance of feldspars. S 4 and some of the samples from S 1 and S 2 also plot along the Fs-FM join. S 4 samples plot closer to the andesites, whereas the S1 and S2 samples plot close to dacite and rhyolite.

The relatively altered rhyolite (CIA=57, Table 2) of Tezuantle Fm. and most of the sediments plot within the feldspar-kaolinite-smectite compositional space. Most of the sediments plots towards the feldspar apex along the Fs-Sm join and some plot above the Fs-Sm join and indicate presence of kaolinite.

DISCUSSION

Tephrostratigraphy and tephrochronology

Stratigraphy of the studied profile suggests at least eigth different events of volcanic eruption in the vicinity of the Pachuca sub-basin ranging in composition from basalt to rhyolite. The tephra layers have different sedimentary and geochemical characteristics. Among the mafic tephra layers, the *ca.* 2.8 m thick basalt to basaltic-andesite Tr 1 is characterised by multilayered lapilli to coarse ash deposits, whereas 0.5 m thick deposits of basaltic-andesite Tr 6 and Tr 7 comprise of fine ash. Compared to both Tr 6 and Tr 7, Tr 1 has higher Ca-bearing pyroxenes and amphiboles and all of them have abundant anorthite (Figures 4a, 4b). The felsic tephra layers are characterised by both massive fine grained ash and grain supported lapilli size pumice fall deposits. Except for Tr 3, the rhyolitic tephra layers are grain supported lapilli size pumice deposits and some even show stratifications, *e.g.* Tr 4. The rhyolitic tephra layers (Tr 3, Tr 4, Tr 5 and Tr 8) have relatively higher abundance of K-feldspar compared to the dacitic ash deposit (Tr 2). Among the rhyolitic tephra, both Tr 4 and Tr 5 have higher Na_2O content compared to Tr 8 possibly related to the presence of glass fragments (Figure 4b).

In order to understand the source of these tephra layers, we compared the bulk rock geochemistry of the tephra layers with the volcanic products from Apan-Tezontepec monogenetic volcanic field (ATVF) (García-Palomo *et al.*, 2002), Acoculco caldera (López-Hernández, 2009), Huichapan caldera (Aguirre-Díaz and López-Martínez, 2009), northern Sierra de las Cruces including La Bufa volcano (Rodríguez-Saavedra, 2007; Quintanilla-Garza, 2008) and Tláloc volcano (Meier, 2007; Roy *et al.*, 2009) located in the surroundings of the Pachuca sub-basin (Table 1 and Figure 3). Both the tephra layers and products from surrounding volcanoes show low to intermediate chemical alteration (CIA < 65). This suggests that the major element geochemistry of both tephra layers and volcanic products represent their original concentrations and hence can be compared. The compositions of the mafic tephra layers (Tr 1, Tr 6 and Tr 7) are comparable to the rocks of ATVF (Figure 3) and because they are typical deposits of monogenetic volcanism (particularly for Strombolian-type eruptions). The rocks forming the ATVF are basalt to basaltic-andesites with aphanitic texture and phenocrysts of olivine and plagioclase (García-Palomo *et al.*, 2002). The position of the mafic tephra layers in the A-CN-K (Figure 4a) and A-CNK-FM (Figure 4c) ternary spaces suggest presence of dominant plagioclase and mafic minerals similar to the deposits of ATVF. The available K/Ar dates from ATVF are 1.50±0.07 Ma (Cantagrel and Robin, 1979), 0.80±0.2 Ma (López-Hernández and Castillo-Hernández, 1997), and 0.47±0.07 Ma (García-Palomo *et al.*, 2002). The tephra layers from the studied profile lack chronological information. As the above mentioned tephra layers are primary fall out deposits and do not have any sedimentological feature showing reworking, they could be correlated to the above mentioned three eruptive events at ATVF based on geochemistry and stratigraphical position. However, the available geochemical data from AVTF do not mention specific ages (García-Palomo *et al.*, 2002). So, we do not correlate the mafic tephra layers to any of the three above mentioned volcanic events, but put the basalt to basaltic-andesite tephra layers in the time interval between 1.5 Ma and 0.47 Ma and the overlying felsic tephra layers as <1.5 Ma.

The rhyolitic tephra layers (Tr 3, Tr 4, Tr 5 and Tr 8) are compared to felsic rocks from Acoculco, Huichapan and Tláloc volcanic structures (Table 1). The chemical compositions of rhyolitic tephra layers and volcanic products from Huichapan and Acoculco calderas are comparable (Figure 3). However, the Huichapan tuff has an older age (4.2±0.2 Ma) and show relatively higher SiO_2 content (Aguirre-Díaz and López-Matínez, 2009) compared to the rhyolitic tephra layers. So, Huichapan caldera as a possible source for any of the rhyolitic tephra layers is ruled out. The rocks of the Acoculco volcanic sequence ranges in compositions from basalt to andesite to rhyolite and were deposited during 3.0–0.24 Ma (García-Palomo *et al.*, 2002) and the felsic rocks (rhyolites) were deposited towards the later part. López-Hernández and Castillo-Hernández (1997) reported the K/Ar date from one of the rhyolites from Acoculco volcanic sequence as 1.7±0.4 Ma. This suggests that the rhyolitic tephra layers at the Pachuca sub-basin are representative of four different volcanic eruptions from the Acoculco caldera that might have occurred after 1.50 Ma and before 0.24 Ma.

The dacitic ash layer (Tr 2) has chemical composition comparable to the products from Acoculco caldera, northern Sierra de las Cruces and Tláloc (Figures 3a and 3b). The felsic deposits of Tláloc are very young (44 ka and 31 ka, respectively) and hence can not be considered as a possible source. There exists a mismatch between Tr 2 and products from Sierra de las Cruces in some of the bi-variate scattered plots (Figures 3d and 3e). Compared to the products from Sierra de las Cruces, Tr 2 show lower concentrations of CaO and MgO. This can be explained by its CIA (51-62) and PIA values (51-66) showing relatively higher chemical alteration compared to products of Sierra de las Cruces (CIA = 48-50). So the mobile and soluble elements like Ca

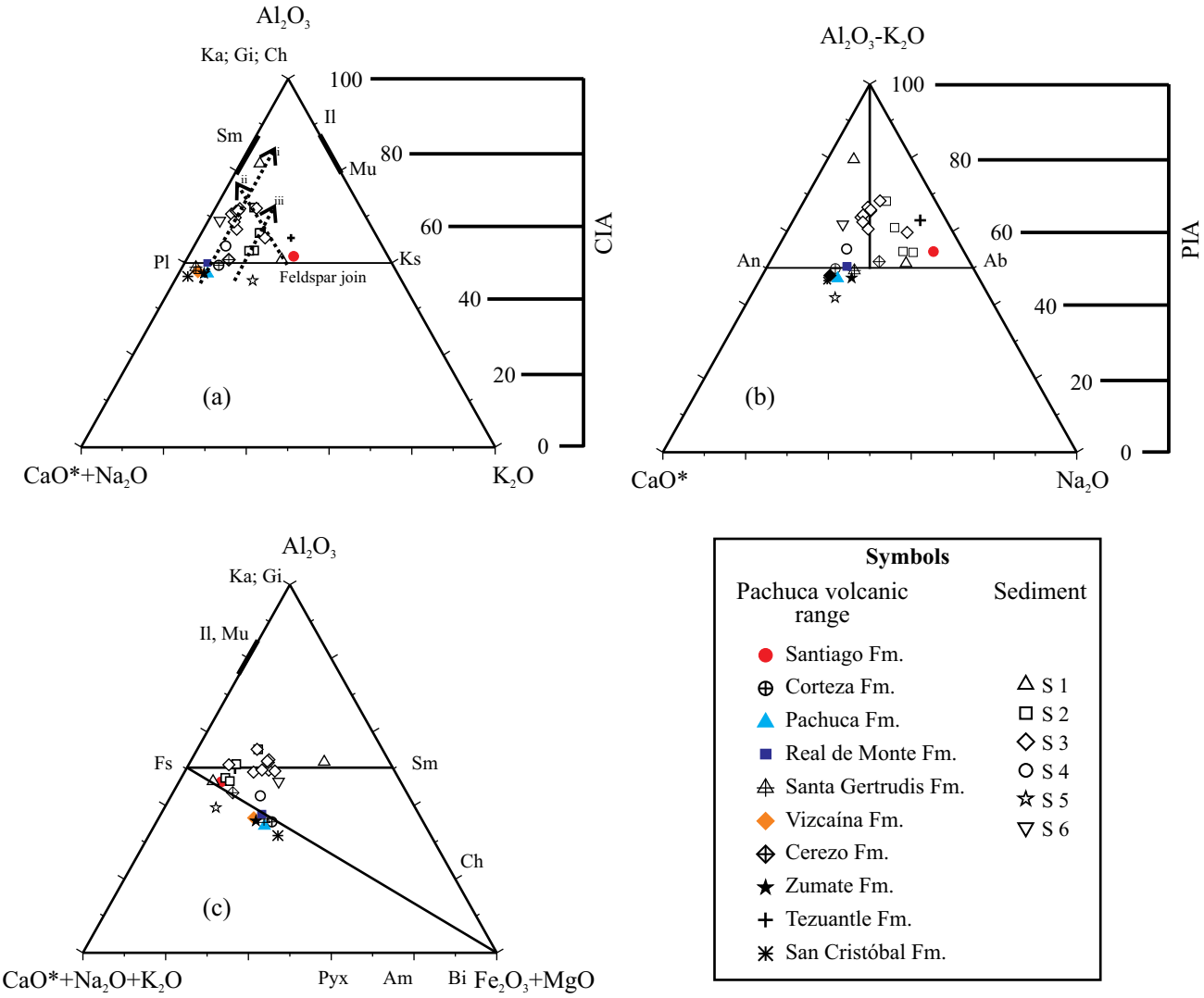

Figure 5. (a) Major element compositions of inter bedded sediments and rocks exposed in the Pachuca volcanic range plotted as molar proportions on an Al_2O_3-(CaO*+Na2O)-K_2O (A-CN-K) diagram. Arrows indicate weathering trend of the sediments. (b) Ternary diagram (A-C-N) showing molar proportions of Al_2O_3 (substracting the Al associated with K), CaO* and Na_2O in sediments and rocks exposed in the Pachuca volcanic range. The scale showing the plagioclase index of alteration (PIA) is shown at the right side. (c) Ternary diagram (A-CNK-FM) showing the molar proportions of Al_2O_3, CaO*+Na_2O+K_2O and Fe_2O_3+MgO in sediments and rocks exposed in the Pachuca volcanic range. The diagram represents the fields of idealised minerals: Pl, plagioclases; Ks, K-feldspars; Il, illite; Mu, muscovite; Sm, smectite; Ka, kaolinite; Gi, gibbsite; Ch, chlorite; An, anorthite; Ab, albite; Pyx, pyroxene; Am, amphibole; Bi, biotite; Fs, feldspars.

and Mg are possibly removed during the alteration of primary minerals of Tr 2. The above mentioned interpretation is also supported by bi-variate plots involving insoluble elements, *i.e.* Al_2O_3 and TiO_2 (Figures 3c and 3f) and presence of clay minerals *i.e.* smectite and kaolinite in Tr 2 (Figure 4c). The available K/Ar date constrains the most recent eruption from the northern Sierra de las Cruces and La Bufa volcano at 3.70±0.40 Ma (Osete *et al.*, 2000), which is much older compared to the tephra layers of the studied profile. Apart from that Sierra de la Cruces are located at a larger distance (*ca.* 100 km from the studied profile) compared to the Acoculco caldera (*ca.* 33 km). This suggests that Tr 2 could be the result of a Plinian-type eruption at Acoculco. However, the interpretations presented here are preliminary and a detailed analysis including geochemistry of individual glass shards and radiometric dates would be needed to improve our understanding of the volcanic history in the northern part of the Basin of Mexico.

Provenance of the inter-bedded sediments

The inter-bedded sediments are characterized by different chemical composition and mineralogical association. S 2 shows felsic constituents, *i.e.* K-feldspar (Figure 5a), albite (Figure 5b) and relatively higher abundance of K_2O, Zr, Y, Rb, Th and Pb (Table 2). Similarly, S 4 and S 6 contain dominant mafic constituents, i.e. anorthite (plagioclase)

and higher abundances of TiO_2, Fe_2O_3, CaO, MgO, Sr, Cr, Ni and Cu. S 5 is characterized by presence of Ca-bearing pyroxenes and amphiboles along with plagioclase and K-feldspar. Both S 1 and S 3 are characterized by presence of felsic and mafic constituents.

Comparable concentrations of insoluble major and trace elements (Ti, Zr and Y, Tables 1 and 2) and their position along the same linear trend (Fig 4a) suggest that S 6 could be an altered product of its underlying tephra layer, *i.e.* Tr 6. This is also supported by the fact that CIA value of S 6 is higher compared to its source Tr 6. Similarly, both S 2 and underlying Tr 2 fall along the same linear array and some samples of S 1 and Tr 1 are present along the same linear trend. However, S 1 has an erosive contact with underlying Tr 1 and S 2 shows relatively lower chemical alteration compared to its source, *i.e.* Tr 2. Apart from that the sediments and their underlying tephra layers have different concentrations of trace elements (Rb, Sr, Y, Zr, Nb, V, Cr, Cu, Th and Pb). This rules out that both these sediment layers were derived from chemical alteration of their underlying tephra layers.

The position of rest of the sediments (S 1, S 3, S 4 and S 5) and their underlying tephra layers along different linear trends in the A-CN-K diagram. (Figure 4a) indicate that these sediments are not produced by the chemical weathering of their underlying tephra layers. Presence of all these sediments along different linear trends containing volcanic rocks from Pachuca range (Figures 5a and 5b) suggests that these sediments are possibly derived by the erosion of basaltic-andesite, andesite, dacite and rhyolites exposed along the Pachuca volcanic range.

However, dissimilarity in trace element concentrations between tephra and sediments could also be due to their different geochemical behavior. Immobile elements are enriched and soluble elements are leached away and hence depleted in the sediments during weathering and pedogenesis. So we consider the possibility that some more S layers could be alteration products of underlying tephra layers, without excluding the observation that some have produced as a result of erosion from the surrounding rocks and pedogenesis of the derived material.

Chemical weathering of the inter-bedded sediments

Except for S 5 (CIA and PIA < 50), the sediments show CIA values varying between 53 and 77 and PIA values ranging between 51 and 80. The varying values of indices of alteration are interpreted as indicators of major element changes due to chemical weathering and soil formation that led to conversion of primary feldspars, volcanic glass and mafic minerals to secondary clay minerals (kaolinite, smectite, etc.) and can be used as indicators of chemical weathering at the source terrain. The degree of chemical weathering and composition of siliciclastic sediments are controlled by both climate and tectonism. In S 5, the absence of chemical weathering and preservation of easily weatherable pyroxenes and amphiboles might have been the result of either a very cool or arid climate or some combination of both. Similarly, the lower to intermediate chemical weathering during deposition of rest of the sediments suggest relatively humid and varying climatic conditions at the source terrains. This is also supported by the presence of smectite and kaolinite in some of the sediments and their absence in others (Figures 5c). On the other hand, lower chemical weathering can also be the result of a tectonically active hinterland (upliftment of igneous rocks) causing its erosion at a higher rate (Andersson *et al.*, 2004). The short time span of exposure to weathering (possibly enhanced by erosion or burial of younger sediments) might have led to lower alteration of the deposited sediments at Pachuca sub-basin. In addition, there are various glacial and interglacial periods registered in high resolution late Quaternary paleoclimatic registers during the time span that cover the studied stratigraphy (last 1.50 Ma). However, it is difficult to propose a paleo-climatic reconstruction in the absence of any precise chronological constraint of the studied profile .

CONCLUSIONS

Compared to the southern and central Basin of Mexico, the northern part is relatively less studied. Stratigraphy and multi-element geochemistry of a *ca.* 30 m thick tephra-sediment sequence from the Pachuca sub-basin gives preliminary but important information regarding tephrostratigraphy, tephrochronology, provenance and environmental conditions of the last *ca.* 1.50 Ma from the northern Basin of Mexico. More specifically:

(i) The mafic (basalt to basaltic-andesite) tephra layers represent three distinct eruptions from Apan-Tezontepec monogenetic volcanoes during 1.50-0.47 Ma. Tr 1 with multilayered lapilli to coarse ash scoria fall deposit could be sourced from a nearer structure, while Tr 6 and Tr 7 with coarse to fine ash fall deposits could be from a structure located at a higher distance.

(ii) The felsic tephra layers represent volcanic events during <1.50- >0.24 Ma at Acoculco caldera. The dacitic Tr 2 and rhyolitic Tr 3 comprises of fine ash deposits, whereas rhyolitic Tr 4, Tr 5 and Tr 8 are characterised by grain supported pumice rich lapilli fall deposits. The lapilli grain size and thicknesses (> 1 m) suggest that some of the volcanic events were of large magnitude (probably Plinian-type eruptions).

(iii) The compositions of the sediments with respect to their tephra layers and rocks exposed in the Pachuca volcanic range in the ternary diagrams suggest that some of them are weathering products of underlying tephra layers and rest of the sediments are possibly derived from the erosion of parental materials comparable to the rocks (basaltic-andesite, andesite, dacite and rhyolite) exposed in the Pachuca range. The varying indices of chemical weathering could

be indicative of varying humidity or duration of exposure to different weathering agents during their transportation and deposition in the Pachuca sub-basin.

ACKNOWLEDGEMENTS

PDR and MPJ acknowledge SNI-CONACyT. This work is financially supported by PROMEP-SEP (PROMEP/103.5/05/1919) and CONACyT Ciencias Básicas (83800). Satellite image of the study area was downloaded from the Global Land Cover Facility, University of Maryland (http://glcf.umiacs.umd.edu/index.shtml) and then processed by L. Capra. We are thankful to both the anonymous reviewers and Jesús Martínez-Frías for their critical comments. This is the 51st contribution from Earth System Science Group, Chennai, India.

REFERENCES

Aguirre-Díaz, G., López-Martínez, M., 2009, Geologic evolution of the Donguinyó-Huichapan caldera complex, central Mexican volcanic belt, Mexico: Journal of Volcanology and Geothermal Research, 179, 133-148.

Aitken, M.J., 1985, Thermoluminescence Dating. Studies in Archeological Science: London, Academic Press, 359 pp.

Andersson, P.O.D., Worden, R.H., Hodgson, D.M., Flint, S., 2004, Provenance evolution and chemostratigraphy of a palaeozoic submarine fan-complex: Tanqua Karoo Basin, South Africa: Marine and Petroleum Geology, 21, 555-577.

Bloomfield, K., Sanchez,-Rubio, G., Wilson, L., 1977, Plinian eruptions of Nevado de Toluca volcano, Mexico: Geologische Rundschau, 66, 120-146.

Bonde, A., Murray, A.S., Frierich, W.L., 2001, Santorini: luminescence dating of a volcanic province using quartz?: Quaternary Science Reviews, 20, 789-793.

Caballero, M.M., 1997, The last glacial maximum in the basin of Mexico: the diatom record between 34,000 and 15,000 years BP from Lake Chalco: Quaternary International, 43/44, 125-136.

Caballero, M.M., Ortega-Guerrero, B., 1998, Lake levels since 40,000 years ago at Chalco Lake, near Mexico City: Quaternary Research, 50, 90-106.

Caballero, M., Lozano, S., Ortega, B., Urrutia, J., Macias, J.L., 1999, Environmental characteristics of Lake Tecocomulco, northern basin of Mexico, for the last 50,000 years: Journal of Paleolimnology, 22, 399-411.

Cantagrel, J. M., Robin, C., 1979, K-Ar Dating on the eastern Mexican Volcanic Belt - relations between the andesitic and alkaline provinces: Journal of Volcanology and Geothermal Research, 5, 99-114.

Fedo, C.M., Nesbitt, H.W., Young, G.M., 1995, Unraveling the effects of potassium metasomatism in sedimentary rocks and paleosols, with implications for paleoweathering conditions and provenance: Geology, 23, 921-924.

García-Palomo, A., Macías, J.L., Tolson, G., Valdez, G., Mora-Chaparro, J.C., 2002, Volcanic stratigraphy and geological evolution of the Apan region, east-central sector of the Trans-Mexican Volcanic Belt: Geofisica Internacional, 41, 133-150.

García-Palomo, A., Zamorano, J.J., López-Miguel, C., Galván-García, A., Carlos-Valerio, V., Ortega, R., Macìas, J.L., 2008, El arreglo morfoestructural de la Sierra de las Cruces, México central: Revista Mexicana de Ciencias Geológicas, 25 (1), 158-178.

Geyne, A.R., Fries, C. Jr., Segerstrom, K., Black, R.F., Wilson, I.F., 1963, Geology and Mineral Deposits of the Pachuca-Real de Monte District, State of Hidalgo, Mexico: Mexico city, Mexico, Consejo de Recursos Naturales no Renovables, 203 pp.

Giaccio, B., Isaia, R., Fedele, F.G., Canzio, E.D., Hoffecker, J., Ronchitelli, A., Sinitsyn, A.A., Anikovich, M., Lisitsyn, S.N., Popov, V.V., 2008, The Campanian Ignimbrite and Codola tephra layers: two temporal/stratigraphic markers for the early Upper Palaeolithic in southern Italy and Eastern Europe: Journal of Volcanology and Geothermal Research, 177, 208-226.

González, S., Huddart, D., 2007, Paleoindians and megafaunal extinction in the Basin of Mexico: the role of the 10.5 Ka Upper Toluca Pumice eruption, *in* Grattan, J., Torrence, R. (eds.), Living under the shadow: The cultural impacts of volcanic eruption: California, One World Archeology Series 53, Left Coast Press, 90-106.

González, S., Huddart, D., Bennett, M.R., González-Huesca, A., 2006, Human foot prints in Central Mexico older than 40,000 years: Quaternary Science Reviews, 25, 201-222.

Guevara, M., Verma, S.P., Velasco-Tapia, F.,, Lozano-Santa Cruz, R., Girón, P., 2005, Comparison of linear regression models for quantitative geochemical analysis: Example of X-ray fluorescence spectrometry: Geostandards and Geoanalytical Research, 29, 271-284.

Lamb, A.L., Gonzalez, S., Huddart, D., Metcalfe, S.E., Vane, C.H., 2009, Tepexpan paleoindian site, Basin of Mexico: multi-proxy evidence for environmental change during the late Pleistocene-late Holocene: Quaternary Science Reviews, 28, 2000-2016.

López-Hernández, A., Castillo-Hernández, D., 1997, Exploratory Drilling at Acoculco, Puebla, México: A hydrothermal system with only nonthermal manifestation: Geothermal Research Council Transactions, 21, 429-433.

López-Hernández, A., 2009, Evolución Volcánica del Complejo Tulancingo-Acoculco y su sistema Hidrotermal, estados de Hidalgo y Puebla, México: Mexico D.F., Mexico, Universidad Nacional Autónoma de México, PhD thesis.

López-Hernández, A., García-Estrada, G., Aguirre-Díaz, G., González-Partida, E., Palma-Guzmán, H., Quijano-León, J.L., 2009, Hydrothermal activity in the Tulancingo-Acoculco Caldera Complex, central Mexico: Exploratory studies: Geothermics, 38, 279-293.

Lozano, R., Bernal, J.P., 2005, Characterization of a new set of eight geochemical reference material for XRF major and trace element analysis: Revista Mexicana de Ciencias Geológicas, 22(3), 329-344.

Lozano-García, M.S., Ortega-Guerrero, B., 1998: Late Quaternary environmental changes of the central part of the Basin of Mexico: Correlation between Texcoco and Chalco basins: Review of Palaeobotany and Palynology, 99, 77-93.

Lozano-García, M.S., Ortega-Guerrero, B., Caballero-Miranda, M., Urrutia-Fucugauchi, J., 1993: Late Pleistocene and Holocene Paleoenvironments of Chalco Lake, Central Mexico: Quaternary Research, 40, 332-342.

Meier, M., 2007, Ursprung und Alter der vulkanischen Gesteine des Vulkans Tláloc, Sierra Nevada, Zentralmexiko: Freiburg, Germany, University of Freiburg, Tesis de Maestría.

Metcalfe, S.E., O´Hara, S., Caballero, M., Davies, S.J., 2000, Records of Late Pleistocene-Holocene climatic change in Mexico- a review: Quaternary Science Reviews, 19, 699-721.

Mooser, F., Nairn, A.E.M., Negendank, J.F.W., 1974, Palaeomagnetic investigations of the Tertiary and Quaternary igneous rocks: A paleomagnetic and petrologic study of volcanics of the Valley of Mexico: Geologischen Rundschau, 63, 451-483.

Nesbitt, H.W., Young, G.M., 1982, Early Proterozoic climates and plate motions inferred from major element chemistry of lutites: Nature, 299, 715-717.

Nesbitt, H.W., Young, G.M., 1984, Prediction of some weathering trends of plutonic and volcanic rocks based on thermodynamic and kinetic considerations: Geochimica et Cosmochimica Acta, 48, 1523-1534.

Nesbitt, H.W., Young, G.M., 1989, Formation and diagenesis of weathering profiles: Journal of Geology, 97, 129-147.

Nesbitt, H.W., Wilson, R.E., 1992, Recent chemical weathering of basalts:

American Journal of Science, 292, 740-777.

Newton, A.J., Metcalfe, S.E., 1999, Tephrochronology of the Toluca Basin, central Mexico: Quaternary Science Reviews, 18, 1039-1059.

Ortega-Guerrero, B., Newton, A.J., 1998, Geochemical characterization of late Pleistocene and Holocene tephra layers from the Basin of Mexico, central Mexico: Quaternary Research, 50, 90-106.

Osete, M.L., Ruiz-Martínez, V.C., Caballero, C., Galindo, C., Urrutia-Fucuguachi, J., Tarling, D.H., 2000, Southward migration of continental volcanic activity in the Sierra de Las Cruces, Mexico: palaeomagnetic and radiometric evidence: Tectonophysics, 318, 201-215.

Quintanilla-Garza, J., 2008, Caracterización mineralógica y química de los polos magmáticos del proceso de mezcla en la Sierra de las Cruces, Cinturón Volcánico Mexicano: Linares, Nuevo León, Universidad Autónoma de Nuevo León, Tesis de Licenciatura.

Rodríguez-Saavedra, P., 2007, Caracterización geoquímica de procesos magmáticos en la parte central del Cinturón Volcánico Mexicano: Sierra de las Cruces: Linares, N.L., Mexico, Universidad Autónoma del Nuevo León, Tesis de Maestría.

Roy, P.D., Caballero, M., Lozano, R., Smykatz-Kloss, W., 2008, Geochemistry of Late Quaternary sediments from Tecocomulco lake, central Mexico: implication to chemical weathering and provenance: Chemie der Erde-Geochemistry, 68, 383-393.

Roy, P.D., Caballero, M., Lozano, R., Pi, T., Morton, O., 2009, Late Pleistocene-Holocene geochemical history inferred from Lake Tecocomulco sediments, Basin of Mexico, Mexico: Geochemical Journal, 43, 49-64.

Roy, P.D., Morton-Bermea, O., Hernandez-Álvarez, E., Pi, T., Lozano, R., 2010, Rare earth element geochemistry of the Late Quaternary tephra and volcano-clastic sediments from the Pachuca sub-basin, north-eastern Basin of México: Geofisica Internacional, 49, 3-15.

Rueda, H., Arce, J.L., Macías, J.L., García-Palomo, A., 2006, A ~31 ka Plinian-subplinian eruption at Tláloc volcano, Sierra Nevada, México, *in* Fall Meeting, American Geophysical Union, San Francisco, USA

Rueda, H., Arce, J.L., Macías, J.L., García-Palomo A., 2007, Pyroclastic sequences at the N-NE slopes of Tláloc volcano, Sierra Nevada, central Mexico, *in* a Commemorative Conference, El Chichón volcano: 25 years later,. San Cristóbal de las Casas, Chiapas, México, p.100.

Urrutia-Fucugauchi, J., Martín del Pozzo, A.L., 1993, Implicaciones de los datos paleomagneticos sobre la edad de la sierra de Chichinautzin, Cuenca de México: Geofísica Internacional, 33, 523-533.

Young, G.M., 2001, Comparative geochemistry of Pleistocene and Paleoproterozoic (Huronian) glaciogenic laminated deposits: relevance to crustal and atmospheric composition in the last 2.3 Ga: The Journal of Geology, 109, 463-47

Manuscript received: December 15, 2010
Corrected manuscript received: September 5, 2011
Manuscript accepted: September 7, 2011